Title: **Procedure to perform a validated incremental hole drilling measurement: Application to shot peening residual stresses**

Authors: **E. Valentini, M. Beghini, L. Bertini, C. Santus, M. Benedetti**

DOI Link: https://doi.org/10.1111/j.1475-1305.2009.00664.x

Qualification of the incremental hole drilling method residual stress measure

E. Valentini[a], M. Beghini[b], L. Bertini[b], C. Santus[b]*, M. Benedetti[c]

[a] SINT Technology s.r.l.
Via Giusti, n.229 – 50041 – Calenzano (FI), Italy.

[b] Dipartimento di Ingegneria Meccanica Nucleare e della Produzione. Università di Pisa.
Via Diotisalvi, n.2 – 56126 – Pisa, Italy.

[c] Dipartimento di Ingegneria dei Materiali e delle Tecnologie Industriali. Università di Trento.
Via Mesiano, n.77 – 38050 – Trento, Italy.

Abstract

The paper describes a test rig designed to check and assess the reliability and the accuracy of the fine incremental hole drilling method. An external load produces a controlled linearly through thickness variable uniaxial stress field, known with good accuracy which can be applied and removed at each hole increment. A procedure is presented to separate the contribution of the relieved strains, caused by the external load, and that produced by the residual stresses in the specimen. A significant effect of the definition of the hole zero depth was observed in order to reproduce the reference bending. A procedure for selecting the zero depth was proposed for correctly reproducing the reference stress. A similar correction was also applied to the residual stress measurements. Hole drilling method reproduced the reference bending stress very accurately, moreover, the residual stress distributions were in good agreement with independent X ray diffraction measures.

Keywords
Residual stresses. Shot peening. Hole drilling method. X ray diffraction. Measurement qualification.

*Corresponding author: Ciro SANTUS
ph.: +39 320 4212184
fax: +39 050 836665
e-mail: ciro.santus@ing.unipi.it

Nomenclature

F	Force producing the reference bending.
b	Bending load lever arm.
h	Specimen thickness.
w	Specimen width at the rosette strain gage location.
Φ	Drilling tool diameter.
E	Young's modulus.
ν	Poisson's ratio.
$\varepsilon_i^F(0)$	Measured strain at zero depth under bending.
$i = 1,2,3$	Strain gage grid indicator number.
z_j	Hole depth at the j–th increment.
$\varepsilon_i(z_j)$	Measured strain at the j–th depth increment, without bending load.
$\varepsilon_i^F(z_j)$	Measured strain at the j–th depth increment, with bending load.
Δz_b	Range of the hole depth due to not perfect bottom surface flatness.
$\varepsilon_i^{\mathrm{RS}}(z_j)$	Relieved strain due to Residual Stress.
$\varepsilon_i^{\mathrm{Be}}(z_j)$	Relieved strain due to Bending stress.
$\varepsilon_{i,\mathrm{err}}$	Strain measurement error.
σ_B	Bending stress at the specimen surface.
$\sigma_{11}, \sigma_{33}, \sigma_{13}$	Stress components calculated by the hole drilling method.

1 Introduction

Hole Drilling Method (HDM) is one of the most widely used technique to measure residual stresses. If compared to X ray diffraction method, the HDM is much less expensive and more suitable for in field applications. HDM is usually described as a semidestructive technique, indeed a small hole is produced at the tested component surface, that usually can be tolerated (for example under static loading) or eliminated if necessary (for example under fatigue loading). Trough thickness residual stress distributions are usually not uniform, particularly if residual stresses are induced by surface treatments such as shot peening. Standard ASTM E837–01e1 [1] was limited to uniform residual stresses, however HDM is widely used also for residual stresses with depth gradients. The basic idea is to record the relieved strains after each of a sequence of hole depth increments, and then the residual stress distribution is obtained by solving an inverse problem, which is classically carried out by the integral method [2, 3, 4]. A fundamental contribution was given by the Finite Element (FE) method that allowed to calculate accurate influence coefficients [5, 6] required to solve the inverse problem. The most recent standard ASTM E837–08 [7] takes into account also the non uniform residual stresses problem, suggesting the use of the integral method to calculate the residual stress distribution by means of the influence coefficients available for some strain gage rosette geometries.

It is well known that the HDM can be affected by several kinds of experimental errors and uncertainties [8, 9, 10, 11, 12]. After a round robin test program, Grant et al. published a *good practice* that covers many possible sources of error about the use of the method, including: strain gage measurement error, hole eccentricity, not perfect cylindrical shape of the hole and uncertainty of the zero depth [13]. Schajer and Altus classified the measurement error sources [8]. They showed that strain measurement errors produce stress calculation uncertainties that are independent of the residual stress, while uncertainties in material constant and hole geometry (diameter and incremental depth) produce errors proportional to the residual stress in the measure region. Zuccarello considered the strain gage error and proposed an optimal hole stepping to reduce the strain error

sensitivity to a minimum [11]. He proposed the optimal stepping for different numbers of depth increments. A larger number of depth increments leads to higher spacial resolution, but also to higher strain error sensitivity. Schajer also confirmed the need of a trade off between resolution and error sensitivity [5]. High gradient residual stress would require small step increments, but error sensitivity needs to be carefully considered.
When the HDM was initially proposed for evaluating variable residual stress by the integral method, the hole depth increments and residual stress calculation steps were coincident [3, 4]. Recently, a more general approach has been introduced. The relieved strains are measured after each hole depth increment (*measurement step*), while piecewise spline solutions can be calculated over larger steps (*calculation step*) solving a least squares problem [14, 15, 5, 16]. Each calculation step necessarily includes at least one measurement step, however the distinction between calculation step and measurement step is noteworthy only if each calculation step includes more measurement steps. Under these conditions the least squares solution produces a useful filtering effect that reduces the noise and the random errors. To apply this approach the calibration coefficients has to be obtained by means of influence functions of the depth. General influence functions were obtained for any combination of parameters (material properties, typical kinds of rosette and hole diameter) by Beghini and Bertini [14] elaborating a series of FE elastic simulations for a large variety of configurations. Recently, the hole eccentricity was also included in the inverse problem calculation as an input parameter [16].
The availability of the analytical IFs allows to elaborate even more than 50 incremental steps within the maximum hole depth. It is important to point out that even using small measurement steps and larger calculation steps, Zuccarello's error analysis [11] is still valid in principle. Residual stress distribution needs to be calculated with a much lower resolution stepping, otherwise the method is sensitive to strain measure errors. The advantage is that it is possible to distribute the calculation steps according to the expected residual stress profile, concentrating more steps in those regions where the residual stress function is more complex, thus adapting the calculation stepping to the solution itself. Though residual stress solution is initially unknown, its local properties can be estimated with preliminary calculations. Exploiting this approach at best, Beghini et al. [17] proposed a genetic algorithm to find the solution that selects the calculation steps in the most efficient way. After a first solution obtained with low calculation step resolution, the algorithm generates new series of calculation step distributions, with higher resolutions, and selects those that give the best representation of the solution (lower standard deviation). The algorithm ends when the solution reproduces the strain measurement with a standard deviation equivalent to the estimated strain measurement error. A higher resolution would reproduce just the measurement errors, rather than giving a better representation of the residual stress profile.
The present paper proposes hole drilling measurements of an imposed bending stress, which is linearly variable along the thickness, and three different shot peening treatments that, on the contrary, induce high gradient residual stresses. Using the known bending stress as a reference it was possible to esteem the HDM measure error and obtain a qualification of the residual stress measures.

2 Material and surface treatments

Different shot peening treatments were applied to plates made by high strength aluminum alloy AA 7075 T651, with composition reported in Tab.1.
The T651 heat treatment applied to aluminum alloy 7075 is:

1. solution heat treatment for 30 min at 475 °C;

Mg [%]	Zn [%]	Cu [%]	Mn [%]	Cr [%]
$2.1 \div 2.9$	$5.1 \div 6.1$	$1.2 \div 2.0$	0.30	$0.18 \div 0.28$
Ti [%]	Si [%]	Fe [%]	Others [%]	Al
0.20	0.40	0.50	< 0.2	balance

Table 1: Aluminum alloy 7075 composition.

Composition	Hardness	Bulk density	Young's modulus
ZrO_2 67%, SiO_2 31%	700 HV	2.3 g cm^{-3}	300 GPa

Table 2: Bead material main properties.

2. water quenching;
3. stress relief by uniaxially stretching up to a permanent strain elongation of 2.5%;
4. aging at 120 °C for 6 hours.

As a consequence of the strain hardening Bauschinger effect during the heat treatment, the T651 treatment tensile yield stress was higher than the compressive yield stress. Two tests (uniaxial compressive and uniaxial tensile) were performed on 7075 T651 samples and the relative stress–strain curves are collected in Fig.1.

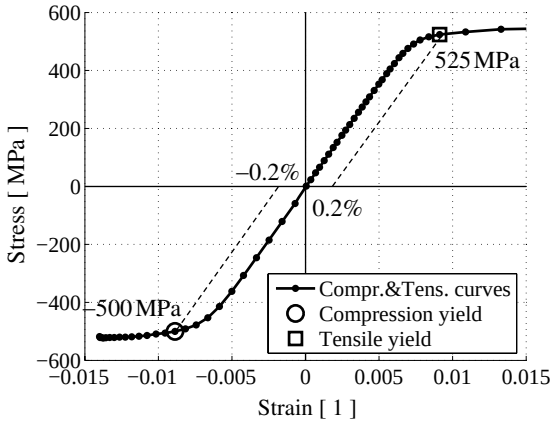

Figure 1: Aluminum alloy 7075 T651 experimental uniaxial (compressive and tensile) tests.

The tensile yield stress was 525 MPa, while the compressive yield stress was -500 MPa (0.2% proof stress).
Both surfaces of each plate were shot peened, and the specimens for the HDM were obtained by milling, after the peening process.
Fused ceramic ZIRBLAST® beads were used for all the shot peening treatments. The ceramic material composition and its mechanical properties are reported in Tab.2. Three shot peening treatments were investigated: the lighter treatment (that is referred to as the B120 treatment) was obtained with small shots, the deeper treatment (Z425 treatment) was obtained with larger shots, and the third treatment (Z425 & B120 treatment) was the Z425 treatment followed by the B120 treatment. The Almen intensities were measured for each treatment, Tab.3.
The microhardness was measured along the specimen depth (Fig.2) in order to show the effects of the surface treatments on the local work hardening that the material experienced. As expected the treatment B120 produced an increase of the microhardness very close to the surface, while the deeper shot peening treatment affected the material properties at higher depth (0.25 mm

Treatment	Bead size [μm]	Bead speed [m/s]	Angle of impingement	Coverage	Almen intensity
B120	$63 \div 125$	57 ± 5	90°	100%	4.5 N
Z425	$300 \div 710$	26 ± 2	90°	100%	4.5 A
Z425&B120	Z425 followed by B120				4.5 A

Table 3: Shot peening parameters.

depth), moreover, the maximum value of the microhardness was found at 0.15 mm depth. For the combined treatment, it is clear that the second peening increases the microhardness within a depth not larger than 0.2 mm, that is exactly the light treatment depth. Considering the increase of the microhardness as compared to the not peened material, the combined treatment microhardness is roughly the superimposition of the two microhardness profiles.

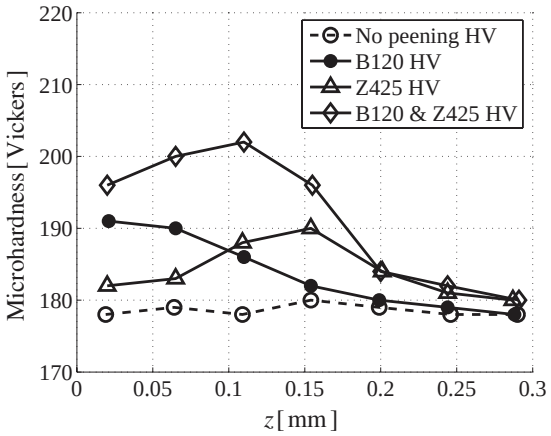

Figure 2: Microhardness profiles for the three shot peening treatments.

2.1 X ray diffraction measurement of shot peening residual stress

X Ray diffraction (XRD) residual stress measurements were carried out using the $\sin^2 \psi$ method [18]. The crystallographic direction $< 422 >$ was chosen in order to obtain high stress sensitivity by means of the Neerfeld Hill method [18, 19, 20]. A specific procedure of chemical etching for the progressive thinning of the specimen was employed [21]. The correction accounting for the effect of the removed layer on the residual stress field was performed according to the indications reported in [18] with the algorithm proposed in [22]. The residual stress field was assumed biaxial, i.e. neglecting the out of plane stress components, and the stresses in the plane were supposed uniform in the XRD sampling volume, which was a spot having a of diameter 2 mm and a depth of $10 \div 30$ μm. The output of the XRD measure is a stress component which is the average between the two in plane principal stresses, however the shot peening is known to introduce an equibiaxial residual stress field. The XRD measurements of the three shot peening surface treatments are reported in Fig.3.

Comparing the microhardness profiles (Fig.2) with the XRD residual stress measures (Fig.3), it is evident that the compressive residual stress depth and the work hardening depth are correlated for the Z425 treatment and for the combined treatment. For both the two treatments the layer depth of the compressive residual stress is 0.25 mm, where the microhardness profile reaches the material untreated microhardness. This correlation is not valid for the B120 treatment, the

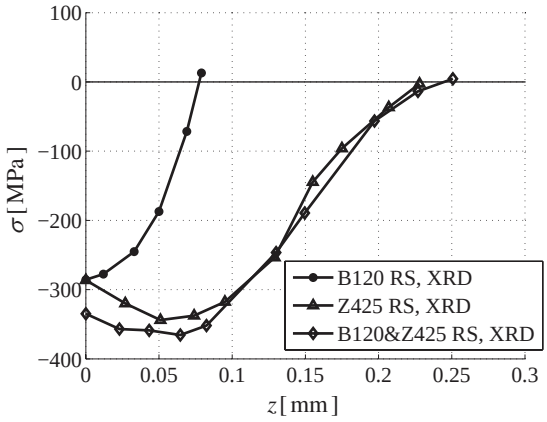

Figure 3: XRD residual stress distributions for the three shot peening treatments.

compressive residual stress depth is 0.075 mm while the microhardness profile is higher than the untreated material microhardness up to 0.150 mm. Coherently, the effect of the B120 treatment superimposed to the Z425 is extended to a depth of 0.2 mm in terms of microhardness profile, and up to 0.1 mm only in terms of residual stress distribution.

3 Bending test rig for hole drilling method qualification

The use of a reference known stress to validate the HDM measure was proposed in the pioneering work by Rendler et al. [23]. Zuccarello also proposed a reference stress measure to have a qualification of the HDM method, by loading a plate specimen under bending, over the yield limit, and then obtaining a residual back stress after removing the load [11]. In order to produce a more controlled stress distribution, to be used as reference, a bending apparatus was designed and manufactured in collaboration between SINT Technology and the Mechanical Department of Pisa University. The apparatus is essentially a cantilever beam, loaded at the free end by a pneumatic actuator force F. When the load is removed, the specimen is under the residual stress only. When the force is applied the specimen experiences the residual stress superimposed to the bending stress. The load is controlled by the cantilever beam stiffness and the actuator stroke, so the load F is applied with good repeatability at every cycle. A load cell allowed to measure the applied load F. The test rig is shown in Fig.4.
The length of the cantilever was chosen in order to produce prevailing bending stress, in the measurement region, and negligible shear stress. As shown in Fig.5(a) the specimen (extracted by the shot peened aluminum alloy 7075 T651 plates) was a part of the cantilever beam. The specimen shape was obtained by milling. The rosette strain gage center was located on the specimen axis in the middle of the tapered region. The angle of the tapered region was chosen in order to avoid longitudinal stress gradient of the prevailing bending stress, as suggested in the standard ASTM E 251–92 [24], Fig.5. Moreover, the distances between the rosette center and the bolted flanges were designed to make the effects of lateral constraint negligible, thus obtaining the bending deformation as a beam structure, in the rosette region. By means of a 3D FE analysis it was verified that the difference between the stress and the prediction by the classical beam theory was below 1%, in the rosette region. Particular care was devoted to the assembly procedure, to avoid misalignments between the specimen axis and the position of the load.

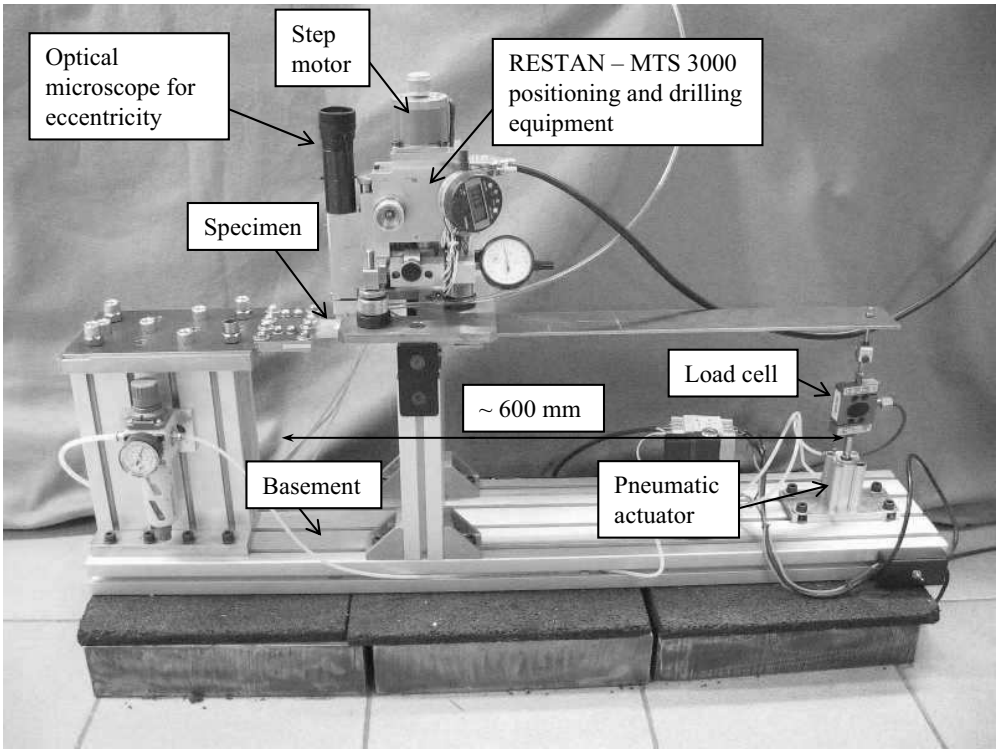

Figure 4: Picture of the test rig and main features.

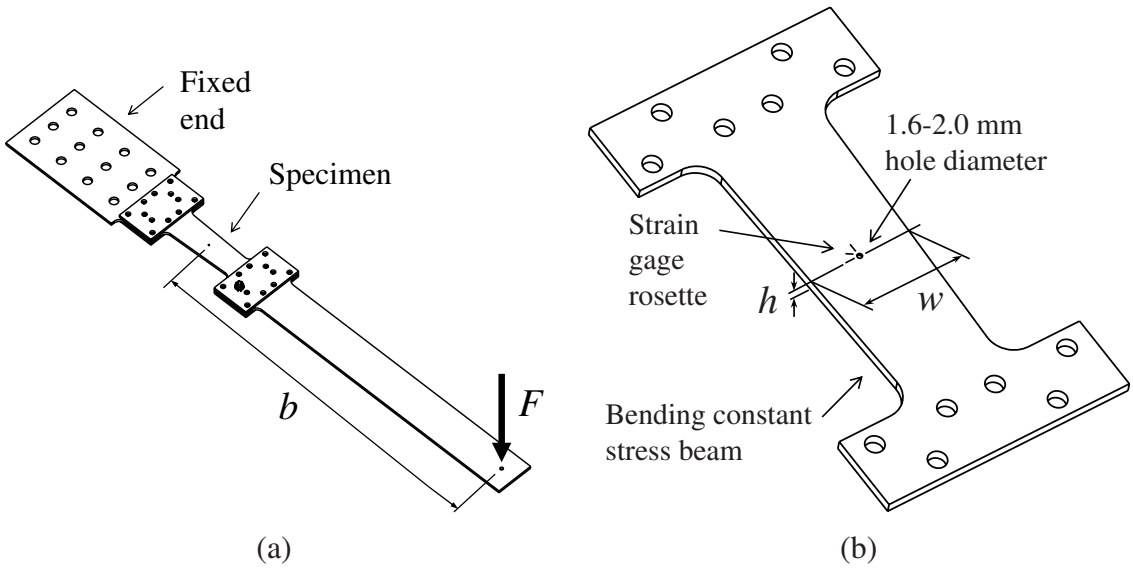

Figure 5: (a) Specimen under bending load. (b) Hole position on the specimen.

3.1 Hole drilling equipment

The hole drilling equipment used in the present experimental activity is produced by SINT Technology srl (that is referred to as 'RESTAN – MTS 3000' in Fig.4), more information is available in Refs.[25, 26]. Details of the hole drilling equipment are reported in Tab.4.
The holes were produced by means of a high speed air turbine (rotational speed: 400 000 rpm) with TiAlN surface treatment carbon tungsten drilling tool. This high speed hole drilling technique was initially suggested by Flaman and Herring [27]. The eccentricity was reduced through a monocular optical microscope with cross hairs to help the operator in aligning the drilling axis

Tool	Model	Company
Strain gage rosette	K–RY61–1S/120R–3–0,5m	H.B.M.
Strain gage amplifier	Spider 8	H.B.M.
Drilling tool	CTT $\Phi = 1.6$ mm	SINT Technology

Table 4: RESTAN – MTS 3000 equipment details.

with the rosette center. After drilling, the effective hole diameter and the residual hole eccentricity were measured using the optical microscope and two micrometric gages (resolution: ± 0.001 mm, uncertainty: ± 0.004 mm) placed on the guides aligned with the rosette axes.

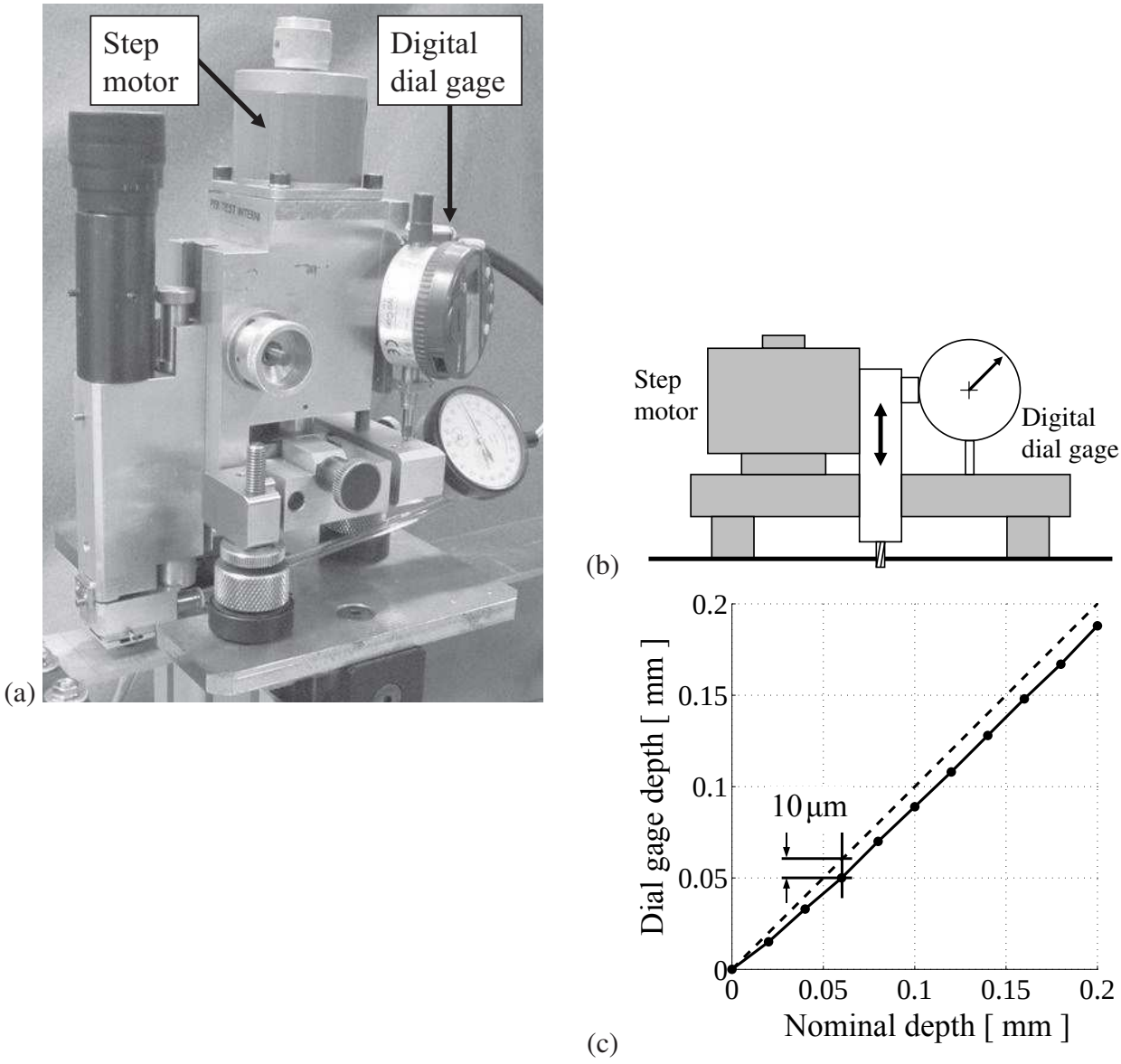

Figure 6: (a) Digital dial gage. (b) Incremental hole depth measure scheme. (c) Dial gage hole depth vs. nominal hole depth.

The zero depth was found by way of an electric contact between the tool and the metallic specimen surface. After the zero depth set up an electric stepping motor drives a calibrated screw system producing the hole depth incremental steps. The actual hole depth increments were also measured by a micrometer with a digital gage indicator (resolution: ± 0.001 mm, uncertainty:

± 0.004 mm), as schematically shown in Fig.6.
The measured hole depth, was slightly different from the nominal hole depth imposed by the step motor, as shown in Fig.6(c). The digital dial gage accumulated an offset in the first few increments, up to 10 μm at the third step (i.e. at the nominal depth of 60 μm), while the following nominal and measured depth increments were in good agreement. The measurement of the depth increments was also verified by optical microscope direct observation of drilled holes, sectioned and polished samples. The hole depth, observed through the optical microscope, was found in agreement with the gage measurement (maximum errors found of few microns), Fig.7.

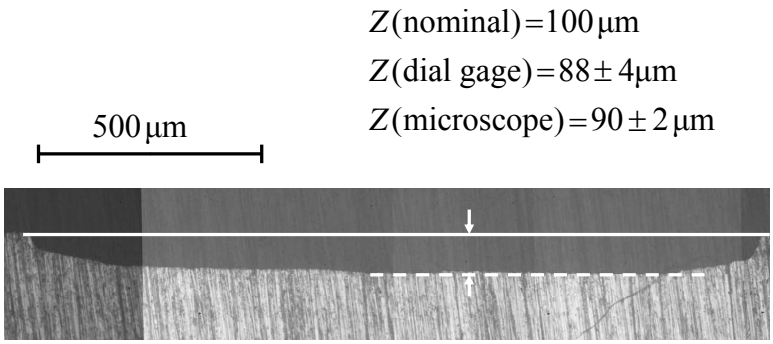

Figure 7: Comparison between the hole nominal depth, the digital gage depth, and the optical microscope direct observed depth.

To produce accurate strain measurements the signal acquisition was repeated 10 times in 0.3 s, and the mean value and the standard deviation were calculated. The strain measurement was performed 3.0 s after each step, in order to extinguish the temperature transient induced by the drilling.
The equipment operating parameters are summarized in Tab.5.

Parameter	Value	Notes
Depth increment speed	0.2 mm/min	
Maximum hole depth	2 mm	
Hole step increment	0.02 mm	Depth range: $0.0 \div 0.5$ mm
Hole step increment	0.05 mm	Depth range: $0.5 \div 2.0$ mm
Strain measure delay time	3 s	
Strain average sampling	10 times after 30 μs each	

Table 5: Operating parameters.

3.2 Testing procedure

The relived strains were measured both with and without the bending stress, after each hole depth increment. To separate the bending stress from the residual stress measures, the following procedure was applied:

1. the signal bridges were balanced with no force applied at the beam;

2. before drilling, the bending load F was applied to the cantilever beam and the rosette strain gage three signals $\varepsilon_i^F(0)$ $(i = 1,2,3)$ were measured;

3. the bending load was removed, verifying that the signals returned to zero;
4. the drilling tool was positioned at the strain gage rosette center (with eccentricity as small as possible, by means of the monocular microscope);
5. the drilling tool was put in contact to the specimen surface, i.e. at the nominal zero depth (with the aid of the electric contact between the specimen surface and the drilling tool);
6. the hole drilling was performed up to depth z_1, without the bending load;
7. the strain signals were measured: $\varepsilon_i(z_1)$, still without the bending load;
8. the bending load was applied and the three strain signals were measured again: $\varepsilon_i^F(z_1)$;
9. the bending load F was removed;
10. steps 6–9 were repeated after each j–th hole depth increment, and signals $\varepsilon_i(z_j), \varepsilon_i^F(z_j)$ were measured (and recorded in a computer file), up to the maximum depth.

The entire procedure was performed automatically by means of a LabVIEW routine programmed on purpose.
Material elastic constants E and ν were found, after the first relieved strain measure $\varepsilon_i^F(0)$:

$$E = \frac{\sigma_B}{\varepsilon_1^F(0)}, \quad \nu = -\frac{\varepsilon_3^F(0)}{\varepsilon_1^F(0)} \tag{1}$$

where the bending stress σ_B is:

$$\sigma_B = \frac{6Fb}{wh^2} \tag{2}$$

Eq.1 is valid if the rosette is oriented with the 1st gage grid aligned with the specimen axis. Fig.5 shows the geometric parameters F, b, w, h.
Measured E and ν were found in good agreement with the expected material constants, Tab.6. This confirmed the validity of the strain measurement.

Specimen #	σ_B [MPa]	$\varepsilon_1^F(0)$ [$\mu\varepsilon$]	$\varepsilon_3^F(0)$ [$\mu\varepsilon$]	E [GPa]	ν
1	65.0	902	−266	72.1	0.295
2	83.7	1159	−361	72.2	0.311

Table 6: Material elastic constants deduced from the strain gage measure, before drilling.

The material elastic constants $E = 72$ GPa, $\nu = 0.30$ were inputed in the subsequent HDM residual stress calculations.

3.3 Separation of the residual and bending stress

The HDM inverse problem was applied both to the self equilibrated residual stress and to the externally applied bending stress. When the bending load F is applied, the specimen is under bending stress *plus* residual stress. The Residual Stress and the Bending relieved strain components $\varepsilon_i^{RS}(z_j), \varepsilon_i^{Be}(z_j)$ were to be separated:

$$\begin{aligned} \varepsilon_i^{RS}(z_j) &= \varepsilon_i(z_j) \\ \varepsilon_i^{Be}(z_j) &= \varepsilon_i^F(z_j) - \varepsilon_i(z_j) - \varepsilon_i^F(0) \end{aligned} \tag{3}$$

$\varepsilon_i^{RS}(z_j)$ and $\varepsilon_i^{Be}(z_j)$ were then inputed into the inverse problem analytical procedure to obtain the residual stress and bending stress distributions, respectively. In the second of the Eqs.3 the initial strain (before drilling) $\varepsilon_i^F(0)$ was subtracted from the j–th strain gage signal, because the *relieved* strain is generated by the introduction of the hole, indeed the bending relieved strain at the zero depth is zero: $\varepsilon_i^{Be}(0) = 0$.

3.4 Choice of the calculation step for the inverse problem

The HDM inverse problem is the calculation of the stress distribution below the surface from the strain gage measurements at the hole depth increments. As described in the Introduction, it has been recently introduced the possibility of using calculation steps larger than the measurement steps. In this activity the measurement stepping was not uniform along the entire hole depth. Near the surface, the measurement step increment was 0.020 mm until the hole depth of 0.5 mm (as previously reported in Tab.5) to have a good resolution in the shot peening depth range. After, the measurement step increment was 0.050 until the final hole depth of 1.700 mm. The inverse problem was solved selecting a calculation step every three drilling incremental steps. Therefore each calculation step was nominally 0.060 mm up to 0.5 mm and 0.150 mm after. The dial gage hole depth measure was used for the experimental hole depths. Therefore, the actual calculation steps are not perfectly uniform, however the use of the influence functions does not require an equally spaced hole depth increments sequence. This high resolution stepping was necessary for reproducing the high gradient residual stress generated by the shot peening treatments. A larger calculation step was also investigated, showing not adequate resolution (see results below). Obviously, to reproduce the bending stress, the best choice would be to select one single linear expression of the stress in the whole domain. However, high resolution calculation step was tested on the reference bending stress to be then adopted for reproducing highly variable shot peening residual stress profiles.

4 Measured bending and residual stresses

4.1 Reference bending stress

Bending relieved strain distributions $\varepsilon_i^{Be}(z_j)$ were calculated, according to Eq.3. Among the three signals ($i = 1,2,3$), $\varepsilon_1^{Be}(z_j)$ was the highest in absolute value ($\varepsilon_1^{Be}(z_j)$ was negative, since at the measuring specimen side the bending stress was tensile). To check the trend, the relieved strains were calculated by means of the influence functions, introducing as input the effective hole diameter, eccentricity, and bending stress distribution as the experimental conditions. The first few points of $\varepsilon_1^{Be}(z_j)$ are reported in Fig.8(a) along with the expected relieved strains at the same hole depths. As mentioned above, the *inverse* problem was solved taking a calculation step every three hole depth increments z_j and obtaining a least squares linear spline solution. The calculated HDM stress distribution is shown in Fig.8(b).

It can be concluded that the HDM reproduces the reference bending stress in the depth range $0.05 \div 1.0$ mm, quite correctly. It is well known that the HDM can not be accurate after (approximately) 50% of the hole diameter, because thereafter the increments are far from the surface, so they produce an effect too small to be accurately measured by the strain gage on the surface. About the test shown in Fig.8 the hole diameter was 1.78 mm and the solution was accurate up to 1.0 mm, Fig.8(b).

The strain gage is very sensitive to the material removal close to the surface, so the bad prediction in the depth range $0 \div 0.05$ mm must be differently explained. The HDM measure in this

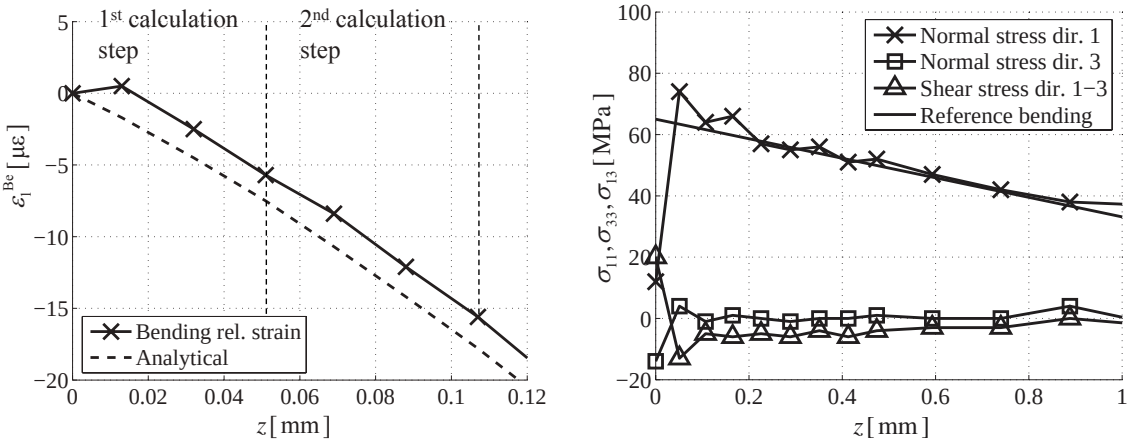

(a) (b)

Figure 8: (a) Bending stress main component relieved strain experimentally obtained compared with the expected trend. (b) HDM reproduced reference bending stress.

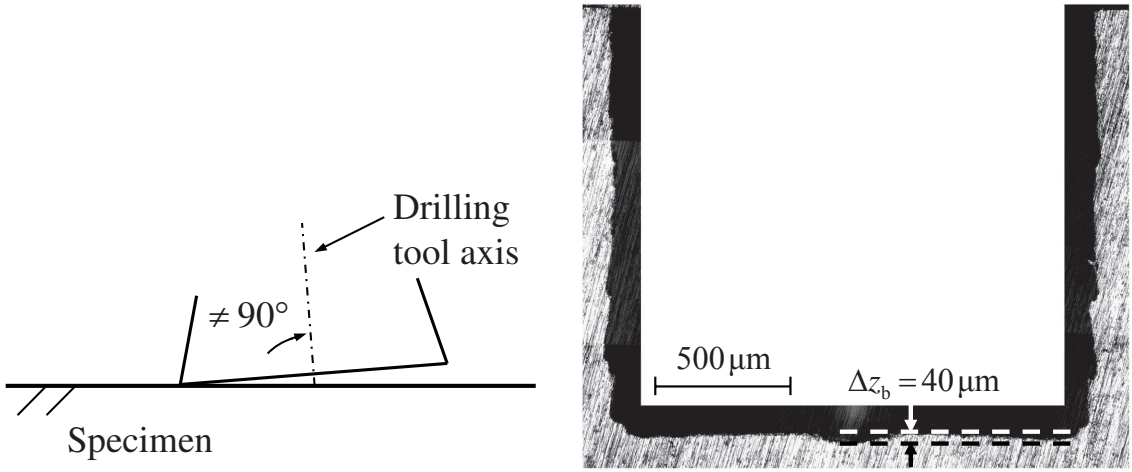

(a) (b)

Figure 9: Section of the hole: (a) not perfect perpendicularity between drilling tool axis and specimen surface (here exaggerated), (b) not perfect flatness of the hole bottom surface.

near surface depth range (that is referred to as the 'subsurface' depth range) is affected by the following sources of error:

- the drilling tool axis perpendicularity with respect to the metal surface can be not perfect, Fig.9(a);
- the hole bottom surface is not planar and it shows a fillet at the edge, the undulation range of the bottom surface $\Delta z_b = 0.04$ mm is comparable with the extension of the first calculation step, where the HDM prediction was inaccurate, Fig.9(b).

During the first hole increment, the cutting edge was not completely in contact with the metal surface (drilling tool axis not perpendicularity), and also the volume of the removed material was not a perfect cylinder (bottom surface undulation and fillet at the edge). As a consequence, the relieved strain signals show a starting point offset. The Fig.8(a) shows an evident zero offset of the first grid signal that was aligned with the bending stress and then measured the highest (absolute value) signal.

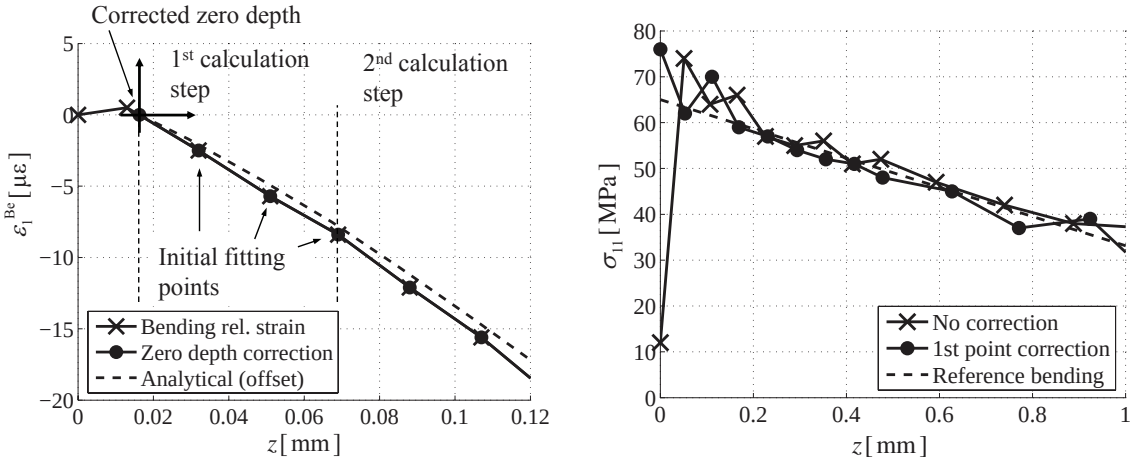

(a) (b)

Figure 10: (a) Linear fit over few initial relieved strains, past the first. (b) Bending stress obtained with corrected relieved strain distribution, compared to the previous result.

After the initial inaccurate measurement, the relieved strain signal keeps increasing with the expected trend, Fig.8(a). This evidence suggests a correction to be performed in order to reduce the zero depth subsurface error. The linear fit interception of few initial relieved strain measurements past the first with the zero strain was assumed as the 'corrected' zero depth and the HDM calculation was performed offsetting the hole incremental depths as shown in Fig.10(a). For the present case the zero depth offset was 0.016 mm, and it produced the effect shown in Fig.10(b). It is evident that before the correction, the estimated subsurface stress was erroneously low, while after the correction the reference bending stress was better reproduced. The zero depth error somewhat propagates over the entire depth range, however its effect was mainly confined to the first calculation step.

It is worth noting that the not perfect flatness of the hole bottom surface is just one source of measure error. Its influence is predominant at the initial steps, but its effect can be coupled with other sources of error. In particular, the strain gage are quite accurate but they can still produce measurement errors, that can be amplified when the HDM inverse problem is solved. According to Figs.11 the maximum error between the bending stress reproduced by the HDM and the reference bending stress is approximately 10 MPa near the surface, though the zero offset correction (without the zero offset the surface error would be much larger). Being the bending stress 65 MPa, the subsurface error is approximately 15% of the expected value.

Performing a difference between the relieved strain, due to the residual stress, and the relieved strain due to the bending, the bending stress relieved strain measurement is then affected by a double strain gage error. Assuming a strain gage error $\pm\varepsilon_{i,\mathrm{err}}$ for each relieved strain independent measure, it follows that:

$$(\varepsilon_i^F(z_j) \pm \varepsilon_{i,\mathrm{err}} - \varepsilon_i^F(0)) - (\varepsilon_i(z_j) \pm \varepsilon_{i,\mathrm{err}}) = \varepsilon_i^{\mathrm{Be}}(z_j) \pm 2\varepsilon_{i,\mathrm{err}} \tag{4}$$

If an acceptable matching is found between the reference imposed bending stress and the stress distribution given by HDM, the accuracy about the residual stress is then expected to be better, because the relieved strain measure is direct. More precisely, considering the linearity between the relieved strain and the calculated stress, the HDM measure uncertainty can be reported on the residual stress measures divided by a factor of 2. An estimate of the subsurface uncertainty is, therefore, $\pm 8\%$ of the surface stress.

Fig.11 also shows the effect of a larger calculation step on the inverse problem solutions. The

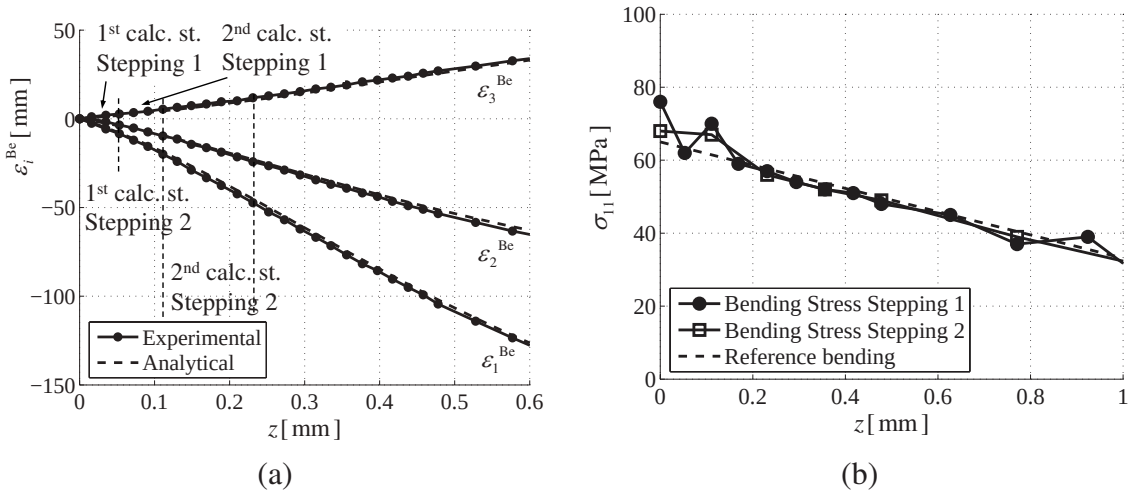

(a) (b)

Figure 11: Reference bending uncertainty sensitivity to the calculation step size.

'Stepping 1' is three measurement steps each calculation step, while the 'Stepping 2' is six measurement steps each calculation step. By using a larger calculation step the error with respect to the reference bending stress was lower. The maximum error reduced to 7 MPa, i.e. 10% of the reference bending stress.
Summarizing the error sensitivity conducted in this section, by means of the reference stress to provide a measure qualification, it was found that:

- in the depth range between the subsurface and (approximately) half the hole diameter, the HDM measure reproduced very accurately the reference bending stress, proving the accuracy of the method;
- a linear fit on initial relieved strains can be used to find a more effective experimental definition of the zero depth, and then the accuracy was improved in the subsurface region;
- though the zero depth correction an error of 15% was still observed in the subsurface depth region;
- considering that the bending relieved strains were the result of the difference of two measures, the subsurface uncertainty to be reported on a residual stress direct measure is $\pm 8\%$;
- by using a double calculation step the subsurface error reduced to 10%, and then the direct measure uncertainty is $\pm 5\%$.

4.2 Residual stress measurements

The zero depth correction was also applied to the measured relieved strain $\varepsilon_i^{\mathrm{RS}}(z_j)$ in order to find the shot peening treatments residual stresses. The shot peening treatments residual stress investigated in the present paper were not expected to be null at the surface, and then the relieved strain were expected to start with a finite derivative (neither zero nor quite low). The zero depth offset corrections were found in the range of: $0.010 \div 0.015$ mm. The relieved strain high derivative assumption does not hold for a generic residual stress field, indeed if the residual stress is low at the surface, the relieved strain does not have an initial high derivative. In such a situation, the relieved strain profile suggests that the zero depth correction can not be applied.
The HDM procedure residual stress results are shown in Fig.12, and they are compared with the XRD measures previously reported, Fig.3.

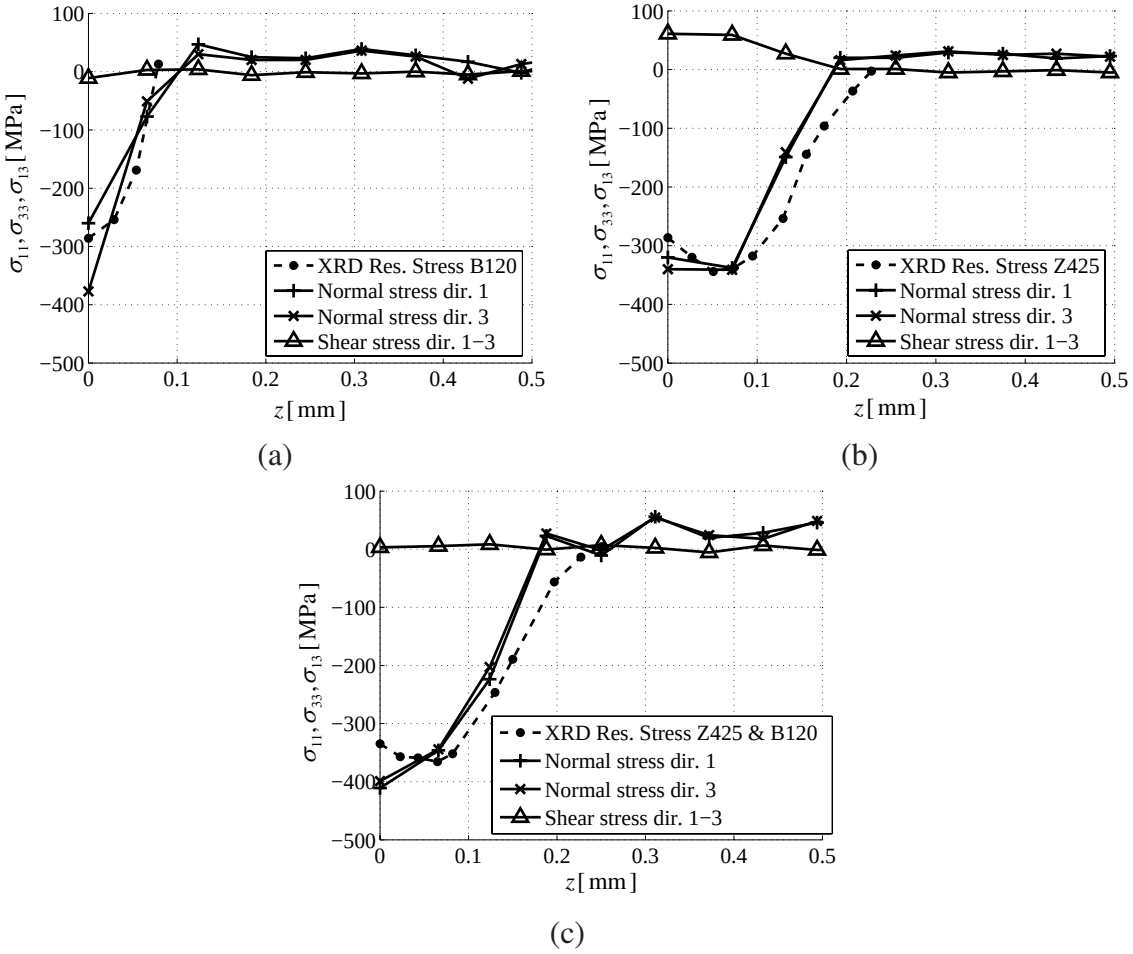

Figure 12: Residual stress measured with HDM and compared with XRD, for the different shot peening treatments: (a) B120, (b) Z425, (c) Z425 & B120.

The HDM procedure output is the three in plane stress components, normal stress along the first grid direction σ_{11}, normal stress along the third grid direction σ_{33}, and finally 1–3 shear stress component σ_{13}. It is evident that the shear stress was negligible in the entire depth range, moreover, the two normal stresses were almost coincident at any depth position, for all the three residual stress distributions. The stress state was then equibiaxial, which is consistent with the shot peening process that does not introduce any preferential direction. Due to the in plane stress equibiaxiality condition the XRD average stress measure was directly comparable to HDM.
In the results reported in Fig.12, the 'Stepping 1' was used (one calculation step every three relieved strain measurements, as discussed above). At the subsurface the estimated uncertainty band is ± 30 MPa (being $\pm 8\%$ of the surface stress: $300 - 350$ MPa, compressive stress), while it is expected to be much more accurate in the depth range 0.050 – 1.0 mm).
The two residual stress measures were essentially in agreement, however, some issues arose that are here discussed. The B120 shot peening treatment was very shallow. The maximum (absolute value) residual stress was found at the surface. It is remarkable that the depth of the layer affected by the residual stress was lower than 0.1 mm, which is just few hole drilling steps, and also similar to the subsurface depth. Though the comparison with XRD is encouraging, a shallow stress distribution, as the B120 treatment, is at the limit of the HDM resolution.
About the deeper treatments (Z425 and Z425 & B120), it is evident that there is a depth offset between the two measures. The depth of the plastic deformation, that produces microhardness higher than untreated material, is correlated to the compressive residual stress depth produced

by shot peening [28, 29]. The HDM measures show compressive residual stress up to 0.2 mm, which is the same depth of Z425 and Z425 & B120 higher microhardness, Fig.2. The chemical etching to produce in depth XRD measure can be a source of depth uncertainty.
The HDM predicts the maximum residual stress at the surface for the Z425 & B120 treatment, while the XRD predicts the maximum residual stress at $0.05 \div 0.08$ mm depth. As discussed above the HDM uncertainty is mainly at the surface, though the zero depth offset correction. An other possible reason of this discrepancy can be the plasticity effect. If the residual stresses are high, the material experiences plastic strain after introducing the hole, and the measured relieved strain are larger than those expected if the material were elastic. The residual stresses obtained by the inverse problem calculation are therefore overestimated. The HDM measure is acceptable only if the stress result does not exceed one half of the yield strength, according to the ASTM standard [1]. Beghini et al. [30] demonstrated that this restriction is overconservative, showing that the measure can be accepted even when the stress result is $60\% \div 70\%$ of the yield stress, expecially for materials with a not negligible strain hardening at the plasticity onset. The shot peening residual stress peak value of 400 MPa, equibiaxial compressive[1] is 80% of the compressive yield stress 500 MPa, Fig.1.
As discussed before, less sensitivity to the strain gage error measure can be obtained with a larger calculation step. However, a drawback is that the spacial resolution can become inadequate to reproduce a complex variable residual stress profile. To investigate this issue through an example, Fig.13 shows the Z425 & B120 residual stress result obtained with the 'Stepping 1': one calculation step each *three* relieved strain steps, as in the results shown in Fig.12, compared to the residual stress result obtained with the 'Stepping 2': one calculation step each *six* relieved strain steps.

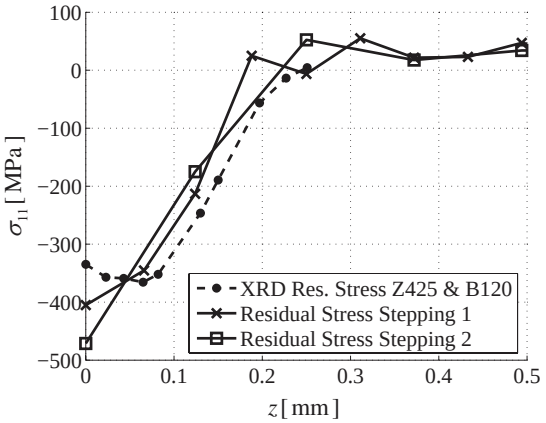

Figure 13: Shot peening treatment Z425 & B120 residual stress distribution, reproduced with a larger (double) calculation step.

The Stepping 2 solution of the Z425 & B120 residual stress measure reported in Fig.13, introduces a maximum resolution error that is approximately 150 MPa, that invalidates the less error strain gage error sensitivity.
In summary the 'best' calculation step choice is to be adapted to the obtained solution. If the residual stress changes remarkably a small calculation step is necessary, despite the higher error sensitivity. On the contrary, for an almost uniform residual stress profile a large calculation step can be used with the benefit of a small strain gage error sensitivity.

[1]The out of plane stress component is null at the free surface, and very low below the surface too. The three principal stress are: $\sigma_1 = -400$ MPa, $\sigma_2 = -400$ MPa, $\sigma_3 = 0$ MPa, therefore the equivalent von Mises stress is $\sigma_{vM} = 400$ MPa.

5 Conclusions

1. A dedicated apparatus was produced to verify the hole drilling method measurement by means of a reference bending stress distribution, which was imposed under controlled conditions and then was known with good accuracy.

2. The bending stress distribution was successfully reproduced by the HDM measure, in the depth range $0.05 \div 1.0$ mm (hole diameter: 1.78 mm). It was verified that the hole drilling method can not accurately measure after a depth approximately 50% of the hole diameter, moreover less accurate measures can also be obtained near the surface.

3. It is here demonstrated that the lower measurement accuracy near the surface was primarily due to the not flat bottom surface of the drilled hole. Indeed, the size of the hole bottom surface undulation was similar to the depth of the less accurate measures near the surface.

4. A simple and quite effective way to reduce this problem was suggested in the paper. If the residual stress at the surface is not negligible, the initial measurement relieved strains have a linear trends that can be captured, with a numerical fit, and then a corrected zero depth can be obtained. The measurement of the reference bending stress was quite improved by performing this correction.

5. The same correction was also applied to the residual stress measurements of shot peened specimens with different intensities. The residual stress distributions were also measured by means of X ray diffraction technique, and a satisfactory comparison was obtained.

6. Using larger calculation steps reduced the maximum error, with respect to the reference bending, but the spacial resolution was obviously coarser. Reproducing a linear variable reference stress with a linear spline, no resolution issue arose. On the contrary, about the shot peening residual stress distribution it was shown that a too large calculation step generated poor resolution error, and then the less strain gage error sensitivity benefit vanished.

Acknowledgments

The authors are grateful to M. Bandini from Peenservice srl, Bologna Italy, for his work to perform the surface treatments shown in the paper, and for the information about shoot peening parameters, and to A. Benincasa from SINT Technology srl for his work to produce the hole drilling experimental results.

References

[1] *Standard Test Method for Determining Residual Stresses by the Hole–Drilling Strain–Gage Method*, 2001. ASTM E837-01e1.

[2] J. Lu. *Handbook of Measurement of Residual Stresses*. Society for Experimental Mechanics, 1996.

[3] G.S. Schajer. Measurement of Non-Uniform Residual Stresses Using the Hole-Drilling Method. Part I - Stress Calculation Procedures. *Journal of Engineering Materials and Technology*, 110:338–343, 1988.

[4] G.S. Schajer. Measurement of Non-Uniform Residual Stresses Using the Hole-Drilling Method. Part II - Practical Application of the Integral Method. *Journal of Engineering Materials and Technology*, 110:344–349, 1988.

[5] G.S. Schajer. Hole–Drilling Residual Stress Profiling With Automated Smoothing. *Journal of Engineering Materials and Technology*, 129(3):440–445, 2007.

[6] J.N. Aoh and C.S. Wei. On the Improvement of Calibration Coefficients for Hole–Drilling Integral Method: Part I–Analysis of Calibration Coefficients Obtained by a 3–D FEM Model. *Journal of Engineering Materials and Technology*, 124(2):250–258, 2002.

[7] *Standard Test Method for Determining Residual Stresses by the Hole-Drilling Strain-Gage Method* , 2008. ASTM E837-08.

[8] G.S. Schajer and E. Altus. Stress calculation error analysis for incremental hole-drilling residual stress measurements. *Journal of Engineering Materials and Technology*, 118(1):120–126, 1996.

[9] D. Stefanescu, C.E. Truman, D.J. Smith, and P.S. Whitehead. Improvements in Residual Stress Measurement by the Incremental Centre Hole Drilling Technique. *Experimental Mechanics*, 46(4):417–427, 2006.

[10] D. Vangi. Data management for the evaluation of residual stresses by the incremental hole drilling method. *Journal of Engineering Materials and Technology*, 116(4):561–566, 1994.

[11] B. Zuccarello. Optimal calculation steps for the evaluation of residual stress by the incremental hole drilling method. *Experimental Mechanics*, 39(2):117–124, 1999.

[12] J.N. Aoh and C.S. Wei. On the Improvement of Calibration Coefficients for Hole–Drilling Integral Method: Part II–Experimental Validation of Calibration Coefficients. *Journal of Engineering Materials and Technology*, 125(2):107–115, 2003.

[13] P.V. Grant, P.D. Lord, and P.S. Whitehead. *The measurement of residual stresses by the incremental hole drilling technique*. National Physical Laboratory, 2002. Measurement good practice guide 53.

[14] M. Beghini and L. Bertini. Analytical influence functions for variable residual stress measurement by the hole drilling. *The Journal of Strain Analysis for Engineering Design*, 35(2):125–135, 2000.

[15] V. Fontanari, F. Frendo, T. Bortolamedi, and P. Scardi. Comparison of the Hole-drilling and X–Ray Diffraction Methods for measuring the residual stresses in shot peened Al–alloys. *Journal of Strain Analysis for Engineering Design*, 40(2):199–200, 2005.

[16] M. Beghini, L. Bertini, and L. F. Mori. General methods for evaluating nonuniform residual stress by the hole drilling method with centered and eccentric holes. *International Journal of Solids and Structures*, 2008. Accepted.

[17] M. Beghini, L. Bertini, and W. Rosellini. Genetic algorithms for variable through thickness residual stress evaluation. In *5th European Conference on Residual Stresses*, pages 145–149, September 1999. Noordwick, Netherlands.

[18] I.C. Noyan and J.B. Cohen. *Residual stress measurement by diffraction and interpretation*. Springer–Verlag New York, 1987.

[19] P.S. Prevey. X–ray diffraction characterisation of residual stresses produced by shot peening. In IITT-International, editor, *Shot peening theory and application*, 1990. Gournay sur Marne, France.

[20] Y.H. Dong and P. Scardi. Marq x–new program for whole powder pattern fitting. *Journal of Applied Crystallography*, 33:184–189, 2000.

[21] M. Benedetti, T. Bortolamedi, V. Fontanari, and F. Frendo. Bending fatigue behaviour of differently shot peened al 6082 t5 alloy. *International Journal of Fatigue*, 26:889–897, 2004.

[22] *Residual stress measurement X–ray diffraction*, 2nd edition, 1971. SAE J 784a.

[23] N.J. Rendler and I. Vigness. Hole–Drilling Stain–Gauge Method of Measuring Residual Stresses. *Experimental Mechanics*, 6(12):577–586, 1966.

[24] *Standard Test Methods for Performance Characteristics of Metallic Bonded resistance Strain Gages*, 2003. ASTM E 251-92.

[25] E. Valentini. An automatic system for measuring non-uniform residual stress by the hole drilling method. In *XIII IMEKO World Congress*, pages 1904–1909, September 1994. Torino, Italy.

[26] E. Valentini, M. Benedetti, V. Fontanari, M. Beghini, L. Bertini, and C. Santus. Fine increment hole–drilling method for residual stress measurement, proposal of a calibrating apparatus. In *Proceedings of the 13th International Conference on Experimental Mechanics (ICEM 13)*, 2007. Alexandroupolis, Greece.

[27] M.T. Flaman and J.A. Herring. Ultra high speed center hole technique for difficult machining. *Experimental Techniques*, 10(1):34–35, 1986.

[28] J. Schwarzer, V. Schulze, and O. Vöhringer. Finite Element Simulation of Shot Peening – A Method to Evaluate the Influence of Peening Parameters on Surface Characteristics. In L. Wagner, editor, *Shot Peening, Proceedings ICSP–8*, pages S. 508–515, 2003. ISBN 3-527-30537-8.

[29] J.P. Nobre, A.M. Dias, J. Gibmeier, and M. Kornmeier. Local Stress–Ratio Criterion for Incremental Hole–Drilling Measurements of Shot-Peening Stresses. *Journal of Engineering Materials and Technology*, 128(2):193–201, 2006.

[30] M. Beghini, L. Bertini, and P. Raffaelli. Numerical Analysis of Plasticity Effects in the Hole–Drilling Residual Stress Measurement. *Journal of Testing and Evaluation*, 22(6):522–529, 1994.

Figures in colors for the on line version of the paper

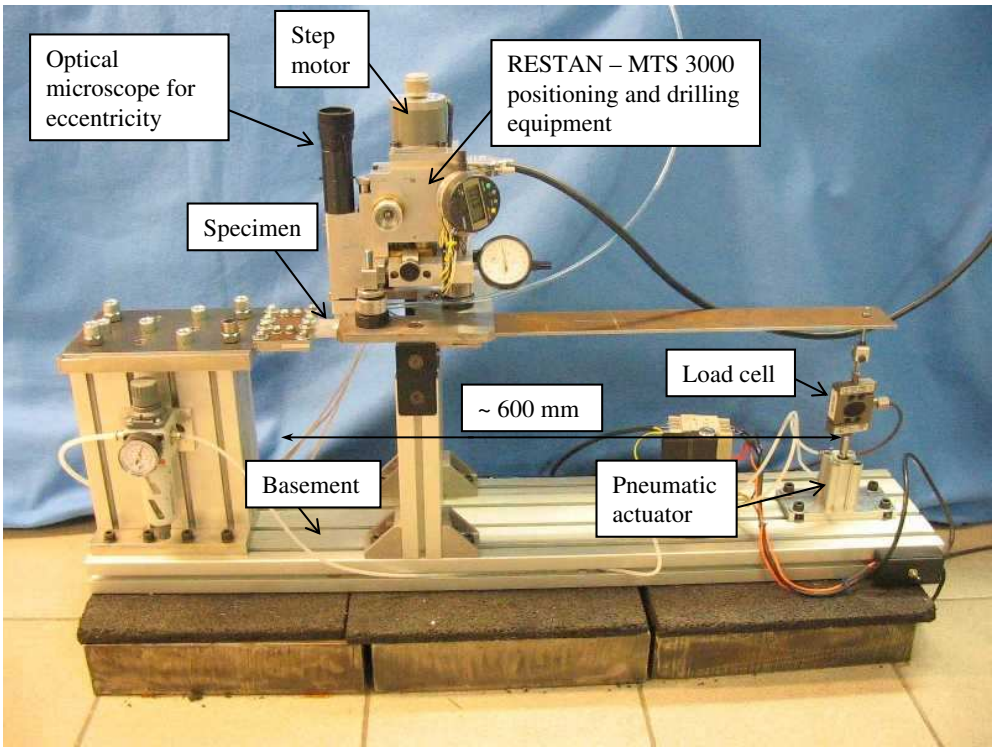

Fig.4 in colors.

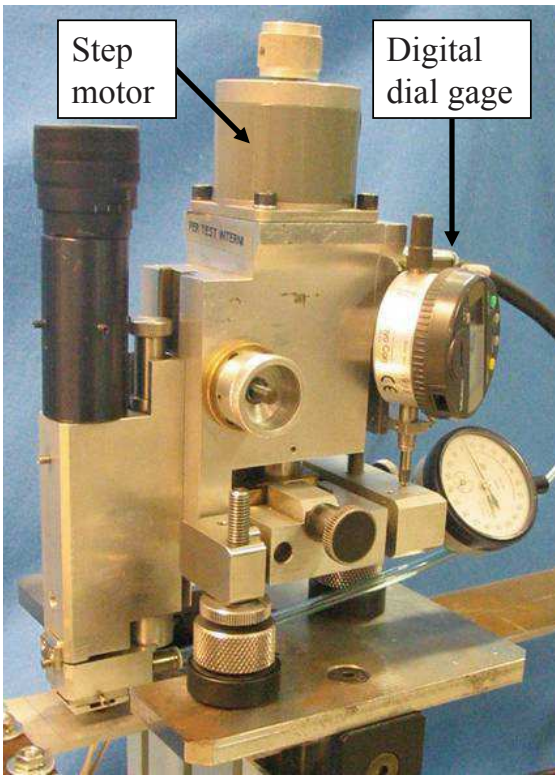

Fig.6(a) in colors.